THE UNIVERSITY of EDINBURGH

Edinburgh Research Explorer

Hydrodynamics of three slender models resembling Polynesian canoe hulls

Citation for published version:
Flay, RGJ, Viola, IM & Irwin, GJ 2019, 'Hydrodynamics of three slender models resembling Polynesian canoe hulls', Paper presented at SNAME 23rd Chesapeake Sailing Yacht Symposium, CSYS 2019, Annapolis, United States, 15/03/19 - 16/03/19.

Link:
Link to publication record in Edinburgh Research Explorer

Document Version:
Early version, also known as pre-print

General rights
Copyright for the publications made accessible via the Edinburgh Research Explorer is retained by the author(s) and / or other copyright owners and it is a condition of accessing these publications that users recognise and abide by the legal requirements associated with these rights.

Take down policy
The University of Edinburgh has made every reasonable effort to ensure that Edinburgh Research Explorer content complies with UK legislation. If you believe that the public display of this file breaches copyright please contact openaccess@ed.ac.uk providing details, and we will remove access to the work immediately and investigate your claim.

OPEN ACCESS

Download date: 12. Oct. 2024

THE 23RD CHESAPEAKE SAILING YACHT SYMPOSIUM
ANNAPOLIS, MARYLAND, MARCH 2019

Hydrodynamics of Three Slender Models Resembling Polynesian Canoe Hulls

Richard G.J. Flay, University of Auckland, Auckland, New Zealand
Ignazio Maria Viola, Institute for Energy Systems, University of Edinburgh, United Kingdom
Geoffrey J. Irwin, University of Auckland, Auckland, New Zealand

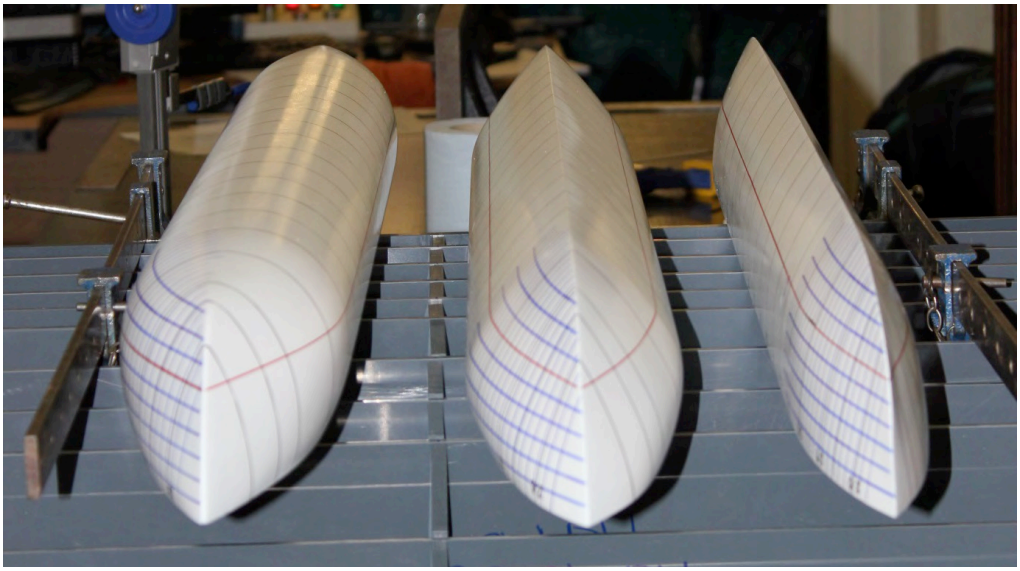

ABSTRACT

Towing tank tests were carried out on three slender models in the Towing Tank at Newcastle University at fixed sink and trim in order to obtain more information on the hydrodynamics of such shapes, and in particular, how the shapes could generate side force when operating at a leeway angle. The research was motivated by a study of ancient Polynesian multi-hull vessels which did not appear to have keels, and so the side-force had to be generated by the hulls. The authors speculate that the earliest vessels had rounded hulls (from trees) and were probably used mainly for sailing downwind. However, it appears that evolution has caused a change in shape from circular to Vee, presumably because such shapes are better able to generate side force to enable the vessels to also sail across the wind.

A CFD study with ANSYS-CFX using three different hulls was carried out as suggested by the first author and it showed that sharper Vee sections were better at generating side-force than a rounded hull. The purpose of the present tests was to investigate whether such behaviour could also be observed in physical testing. Three models were manufactured and were tested in the Towing Tank at Newcastle University in July and August 2013.

It was found that there was good agreement between the CFD and tank test results, and that indeed the hypothesis that narrower Vee-shaped hulls would generate more side-force when at leeway than a rounded hull was proved.

INTRODUCTION

This work was carried out while the first author was on Sabbatical Leave at Newcastle University during May to September 2013, and it was one of the Work Packages in the Sailing Fluids research project, funded by the Marie Curie International Research Staff Exchange Scheme (FP7 IRSES) and by the Royal Society of New Zealand.

Towing tank tests were carried out on three slender models in order to obtain more information on the hydrodynamics of such shapes, and in particular how the shapes could generate side force when operating at a leeway angle.

Slender hulls are of much interest for multi-hull vessels. There is increased interest in such vessels at present due to the use of wing-sail multi-hulls in the recent 2013 America's Cup races in San Francisco, although the AC yachts use foils to generate a lot of the side force, and only at low speeds are the hulls in the water. On the other hand, ancient Polynesian multi-hull vessels did not appear to have keels, and so the side-force had to be generated by the hulls. The authors speculate that the earliest vessels had rounded hulls (from trees) and were probably used mainly for sailing downwind. However, with time, it would have been realised that sail powered vessels could also manoeuvre across the wind, and then the importance of side force as well as drag would have begun to be appreciated. Modern Polynesian multi-hull vessels often have one or both hulls which are Vee-shaped in cross-section. Hence it appeared that evolution may have caused a change in shape from circular to Vee, presumably because such shapes are better able to generate side force.

A CFD study with ANSYS-CFX using three different hulls was carried out as suggested by the first author and it showed that sharper Vee sections were better at generating side-force than a rounded hull. The purpose of the present tests was to investigate whether such behaviour could also be observed in physical testing. Three models were manufactured and were tested in the Towing Tank at Newcastle University in July and August 2013. One set of tests were carried out with fixed sink and trim, and the August tests had free sink and trim, with a thrust moment applied which approximated the sail force located partially up the mast. This paper is restricted to discussing the fixed sink and trim tests only.

It was found that there was good agreement between the CFD and tank test results, and indeed that the hypothesis that narrower Vee shaped hulls would generate more side-force when at leeway than a rounded hull was proved.

This work was primarily motivated by two objectives: first, to obtain information on the hydrodynamics of slender hulls that could be used for helping to understand and predict the performance of Polynesian sailing vessels; second, to learn how to use a Towing Tank, as there is not one at the University of Auckland. Thus it was decided that the slender hull tank results would be analysed and written up in a report and paper for their own sake, to add to the literature on such shapes. Also the tests would be used to train University of Auckland academics, students and technicians in the techniques of tank testing. The tests were carried out by Richard Flay, Alexander Blakeley (UOA PhD student), Joshua Taylor (NU Summer student, and Nick Velychko (UOA Technician).

DESCRIPTION OF NEWCASTLE UNIVERSITY TOWING TANK

Since its construction in 1951 the Towing Tank at Newcastle, Figure 1, has been in almost continuous use. Since then, the tank has been regularly updated to keep abreast of modern trends. This includes the fitting of wave making and electronic recording equipment. Recent upgrades include the installation of a state-of-the-art motor control system to enhance very slow speed and high speed testing capabilities. A recent innovation is a modern telemetry system which will allow data to be sampled without any wired connections between the carriage and shore-based equipment. Further details are available in Newcastle Towing Tank, 2018 and Table 1.

Figure 1 Photograph of the Newcastle University Towing Tank

The Towing Tank is used mainly for calm water, wave resistance and sea-keeping experiments. Models are towed using a monorail carriage system that has a maximum speed of 3 m/s in its normal mode. The carriage can be remotely or manually controlled, while the 32-channel data retrieval system is on-line to a PC. The wave-makers can be used to generate regular waves of up to 0.12 m in height and wave periods in the range of 0.5 to 2 seconds. They are also capable of generating long crested random seas using a variety of wave spectra.

Table 1 Towing Tank Specifications

Specifications	
Tank length	37 m
Width	13.7 m
Water depth	1.25 m
Normal Carriage velocity	3 m/s
Wave capability	
Period range	0.5 - 2 Sec
Wave height	0.02 - 0.12 m (Period Dependent)

DESCRIPTION OF THE THREE MODELS

Model Manufacture

The models were based on those used for the CFD investigation by Boeck 2010 and 2012, using ANSYS-CFX, when he was studying in the Yacht Research Unit at the University of Auckland, and CAD images of the three models can be seen in Figure 2. It was decided to manufacture models for tank testing at the University of Auckland, and since the tank was small, and the models had to be shipped to the UK, a scale of 1:10 was used. The CFD investigation used hulls of length 12 m, as advised by Emeritus Professor Geoffrey Irwin, and so the models had an overall length of 1.2 m. Further details of the models are given in Table 2. They are rather small models, and it was realised once the tests were started that it would have been possible to test larger models at yaw, such as 50% longer, but they would have been more difficult to ship from NZ to the UK and back.

Table 2 Model-scale details of the three models used in the CFD and towing tank investigations, Boeck 2010. V1 – rounded hull, V2 – wide Vee, V3 – narrow Vee hull.

	V1	V2	V3
Draft amidships [m]	0.046	0.046	0.046
Waterline length [m]	1.16	1.16	1.16
Keel angle [deg]	180	100	70
Displacement [kg]	3.8	2.1	1.3
Wetted surface area [m^2]	0.163	0.129	0.111
Water plane area [m^2]	0.117	0.085	0.054
WL beam [m]	0.117	0.086	0.054
Prismatic coeff.	0.822	0.823	0.827
Block coeff.	0.492	0.341	0.263
Midship area coeff.	0.753	0.556	0.556
Water plane. Area coeff.	0.867	0.851	0.856
Projected side area [m^2]	0.0488	0.0488	0.0488

Igs files developed in Boeck 2010 were provided to the Faculty of Engineering Workshop, and these files were used to drive a numerically controlled milling machine to cut the shapes out of blue foam (Styrofoam). The foam models were then covered in a layer of fibre glass and painted, to strengthen them and to make them waterproof. A photograph of the models can be seen in Figure 3. The design waterline is shown in red and is the same for all three models. It was decided that the testing would be based on having constant draft, and hence the displacements of the models varied. The projected side area of all models is the same and is 4.88 m^2 in full-scale, or 0.0488 m^2 in model scale.

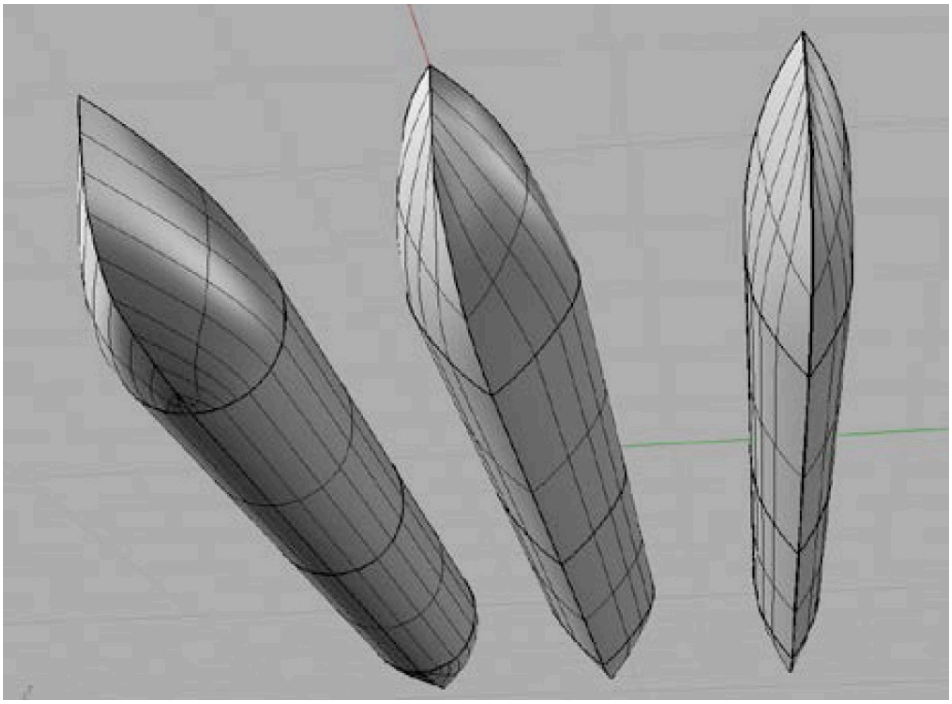

Figure 2 CAD image of the three models used in the CFD investigation from Boeck 2010. Left V1 – rounded hull, Centre V2 – wide Vee, Right V3 – narrow Vee hull

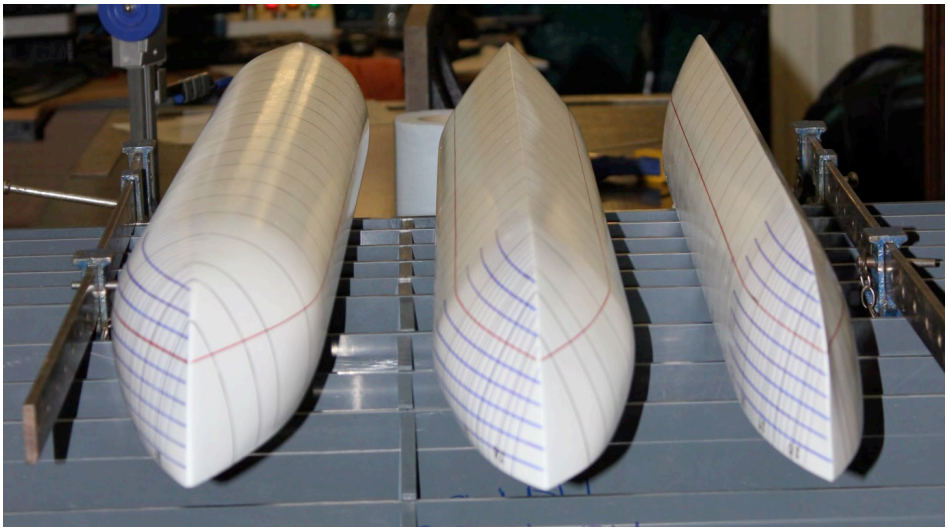

Figure 3 Photograph of the three models showing the underside and the painted grid pattern for assessing wave motion. The water line is shown in red. V1(left), V2(centre) and V3(right).

Model fixture to the Gifford dynamometer

A schematic diagram of the Gifford dynamometer is shown in Figure 4. The heave post is attached to the carriage. For fixed sink and trim tests it is clamped so that the model is immersed to the water line when at rest in still water. The pivot base is also secured with rectangular blocks so that it cannot rotate, and during setup the model attitude is adjusted to horizontal using shims. For free to sink and trim tests, the heave post is free to move vertically under the action of the force transmitted to it by the model and the pivot base is free to rotate. The towing plate is rigidly attached to the model, and its angular position is set by screws through holes at predetermined locations. The towing plates can be seen attached to the models in Figure 5. Holes were pre-drilled into the plates at 2° intervals, and enabled the larger two models to be tested at leeway angles from 0° up to +/- 24°. The narrower V3 model could be tested up to +/- 16°. It was expected that the narrower V3 model would generate more side force for a given leeway angle, which is why it was decided to have a lower maximum leeway angle for

this model, although as can be seen in Figure 5, the maximum angle was also limited by the model width.

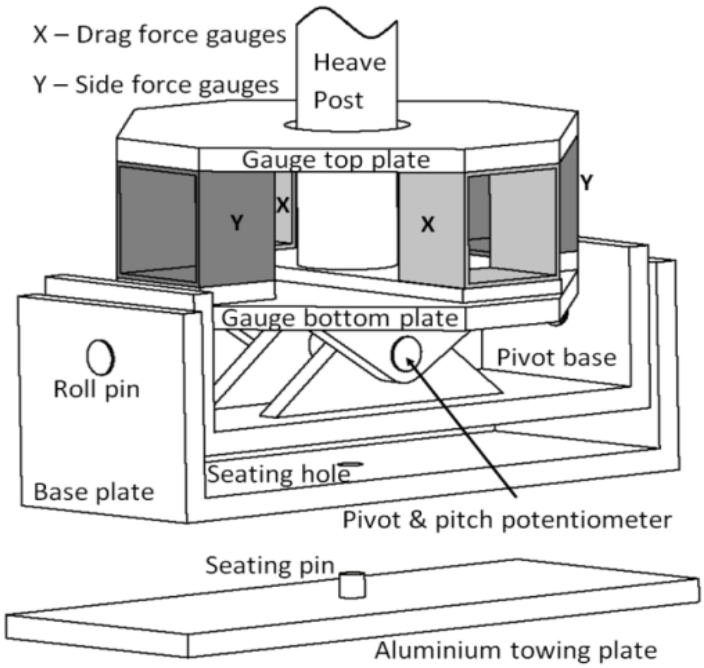

Figure 4 Schematic diagram showing the working principles of the Gifford dynamometer.

Trip wire placement

Trip wires are commonly used on tank test models to fix the location of transition, which would occur further aft at model scale compared to full scale, because of the lower Reynolds number (Re) in the former situation. If we assume that these vessels could travel at say 10 knots or 5 m/s, then based on their length of 12 m, the Reynolds number is: $Re_{fs} = 60$ million, and the Froude number is: $Fr_{fs} = 0.461$.

If we assume that transition occurs at 0.5 million, then this is at $x_{tr} = 12 \times \frac{0.5}{60} = 0.1$ m. As a fraction of the length, this is 0.83%. At 5 knots (half the speed) transition would occur at 0.2 m from the bow, which is 1.6% of the length. Thus in full-scale transition is expected to occur very near the bow. The model scale Reynolds number, Re_m, is much less. At 10 knots $Fr_{fs} = 0.461$, so for a model scale of 1/10th, the equivalent test speed is given by $V_m = 1.58$ m/s, and thus $Re_m = 1.9$ million. Assuming as above that transition occurs at half a million means that it will occur at 26% of the model length, which is a distance of 0.32 m from the bow. Thus the nature of the flow would be very different, and would be likely to lead to errors in viscous drag.

The recommended ITTC 2002, Rev 01 approach was taken to determine the location of a trip wire to fix transition. ITTC recommends that a trip wire be located 5% of the length between perpendiculars (*Lpp)* aft of the forward perpendicular (*FP*), and that the wire diameter be between 0.5 and 1.0 mm. Thus for all three models, the wires were located a distance 58 mm aft of the *FP*, which itself is 20 mm aft of the foremost part of the model, so they were 78 mm aft of the foremost part of the model. Note that it is standard practice at Newcastle to use wire of diameter 1.2 mm, and this wire diameter was used on the three models. This slightly larger diameter than that recommended by ITTC could result in a slight increase in drag. An example of the trip wire on model V2 can be seen in Figure 6. The two other models had trip wires at the same location. Thus the trip wire was located a distance 6.5 % of the model length from the bow, i.e. aft of where one might expect transition to occur in full-scale, but well ahead of where it could be expected to occur naturally at model scale.

Definition of drag, lift, resistance, side-force coefficients

The main model dimensions are given in Table 2. Coefficients are made dimensionless using the product of area and dynamic pressure. The reference area, *A*, is normally the immersed projected side area, which is the same for all three models, and so changes in the coefficients relate directly to forces. For some of the analysis, especially for the drag, sometimes the reference area is the wetted surface area, with the model upright and immersed to its waterline. It is given the symbol *S*. Which reference area is used to form the coefficients is made clear in the relevant text. For example when applying the Prohaska-

Hughes method to relate model to full-scale drag coefficients, it is convenient, and conventional to use the wetted surface area. ρ is the density, and V is the velocity of the model through the still tank water. The International Towing Tank Conference (ITTC) Recommended Procedures (2002) defines density for g = 9.81 m/s^2 as in Eq. (1).

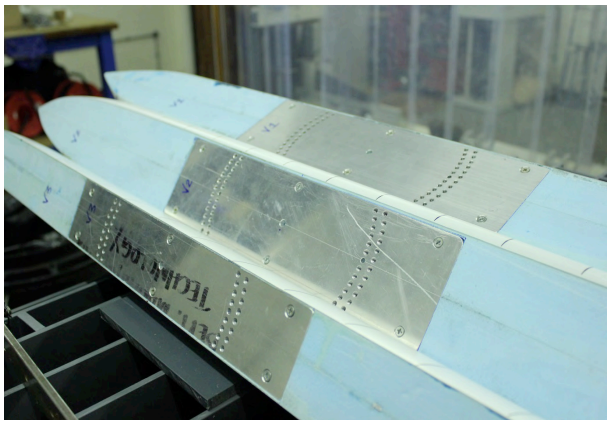

Figure 1 Photograph of models showing attachment of the towing plate with holes pre-drilled at 2° intervals.

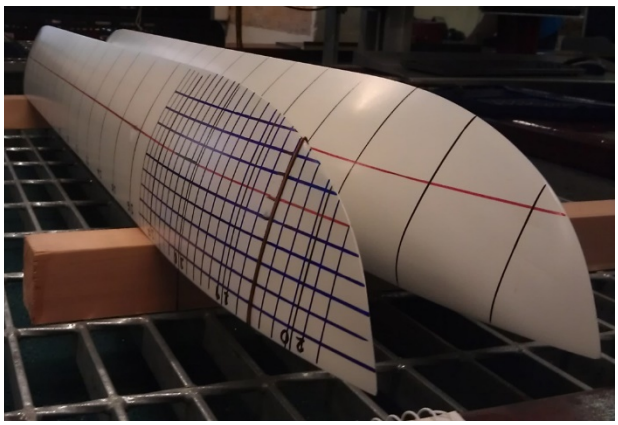

Figure 6 Photograph of model V2 showing the trip wire to initiate transition.

$$\rho = 1000.1 + 0.0552t + 0.0077t^2 + 0.00004t^4 \quad (1)$$

where t is temperature of water in °C.

The coefficients defined herewith are all located in the horizontal plane, normal to gravity.

Drag

Drag is the force in the direction parallel with the onset flow, so in the tank it is the force along the tank axis, and the drag force coefficient is defined in Eq. (2).

$$C_D = \frac{F_D}{\frac{1}{2}\rho A V^2}, C_D = \frac{F_D}{\frac{1}{2}\rho S V^2} \quad (2)$$

Lift

Lift is the force in a direction normal to the onset flow, so in the tank this is the force perpendicular to the tank axis. The lift coefficient is defined in Eq. (3).

$$C_L = \frac{F_L}{\frac{1}{2}\rho A V^2} \quad (3)$$

Resistance

The resistance coefficient is defined here as the force along the longitudinal axis of the model. When there is no leeway it is the same as the drag coefficient. When the model is at a leeway angle λ, the resistance coefficient is related to the drag and lift coefficients as in Eq. (4).

$$C_R = C_D \cos\lambda - C_L \sin\lambda \quad (4)$$

Side force

The side force is normal to the resistance, and the side force coefficient is related to the drag and lift coefficients as in Eq. (5).

$$C_S = C_D \sin\lambda + C_L \cos\lambda \quad (5)$$

PREDICTION OF DRAG AND SIDE FORCE FROM THE CFD INVESTIGATION

A CFD investigation using ANSYS-CFX was carried out by Boeck 2010 and 2012, for his master's thesis while studying in the Yacht Research Unit at the University of Auckland. The aim of the study was to investigate the generation of side force for hull shapes ranging from circular to a narrow Vee. Three model shapes were investigated, as depicted in Figure 2.

Boeck initially modelled the so-called Wigley hull which has been well studied, and for which there are numerous experimental data available. He compared his predictions with the published Wigley results and verified that his CFD modelling appeared to be working well both in terms of the wave height along the hull, and the drag. For example, comparisons in Boeck, 2010 with experimental data from Wong 1994 show that resistance coefficient differences for Froude numbers of 0.225 and 0.267 are less than 0.005, and for a large Froude number of 0.316 the CFD under-predicts the experimental value by 0.03. He then modelled the three hull shapes which were the main subject of the investigation. Predictions of lift and drag

were made at leeway angles of 0, 5, 10 and 15°, at a speed of 1.543 m/s (3 knots) which corresponds to a Froude number of 0.12. He also tried to obtain predictions at the higher speed of 5 m/s, but these runs did not converge to reliable solutions for reasons that are not entirely clear.

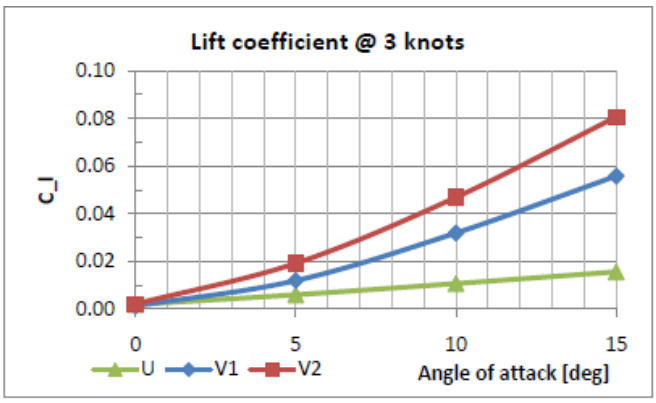

Hydrodynamic lift coefficient

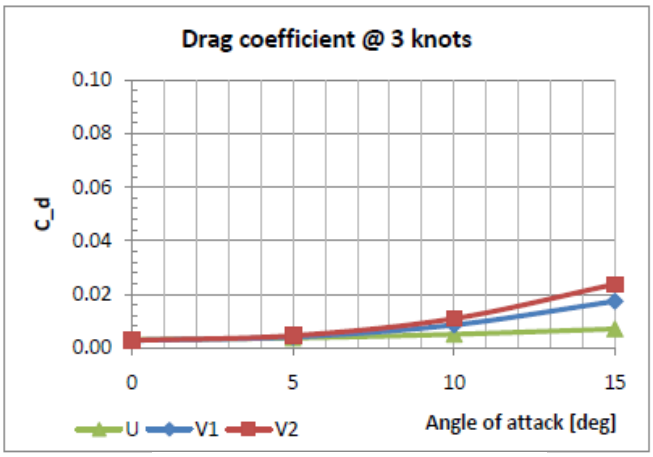

Hydrodynamic drag coefficient

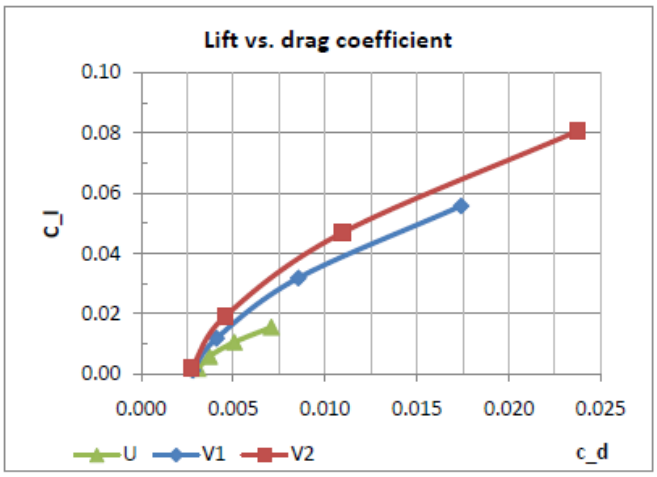

Hydrodynamic lift versus drag coefficient

Figure 7 Drag and lift coefficient predictions by Boeck 2010 using ANSYS-CFX. Note that in this figure U corresponds to the rounded hull, V1 to the wide Vee, and V2 to the narrow Vee. Wetted surface area was used as the reference areas for these hulls. Top: lift coefficient versus angle of attack, centre: drag coefficient versus angle of attack, bottom: lift coefficient versus drag coefficient.

The results available in Boeck 2010 use the wetted surface area of the hull as the reference area, which is different for all the three models. In order to eliminate this variable, it was decided that for the present work the reference area would generally be the immersed projected side area, which is significantly smaller than the wetted area, and would therefore lead to higher force coefficients. The values of the various areas for the models are given in Table 2. The CFD predictions from Boeck 2010 are given in Figure 6 and Table 3.

Table 3 Force and moment predictions using CFD for the narrow Vee hull, from Boeck 2010.

speed [m/s]	AOA [°]	Fx [N]	Fy [N]	Fz [N]	Mx [Nm]	My [Nm]	Mz [Nm]
1.543	0	35.85	26.42	13621.61	18.50	-86.82	-94.27
1.543	5	35.00	250.00	13500.00	200.00	-175.00	-600.00
1.543	10	34.38	629.22	13384.93	451.94	-345.16	-1149.93
1.543	15	27.13	1099.48	13232.65	783.48	-660.20	-1972.66

FIXED SINK AND TRIM TESTS (JULY 2013)

A week of testing time in the tank was available during the period 1-5 July 2013. In order to make the best use of a relatively limited time, it was decided that these tests would be conducted with "fixed sink and trim". This means that the heave post is locked so that the model cannot move vertically, nor pitch. Such tests are simpler to conduct that "free to sink and trim" tests, as the former do not require the pitching moment to be calculated for a given towing force. In addition, these tests were used for the initial training of The University of Auckland staff and student in tank test techniques. The paper does not discuss the free to sink and trim tests.

.

Test schedule

Since the primarily objective of the test programme was to understand how the hull shape affected the lift or side force when the model had various amounts of leeway, a test schedule was prepared which was a matrix of with speeds ranging from 0.4 to 1.6 m/s, and leeway angles from 0 to 24°. As the test progressed, there were changes based on observations of tests, such as the speed and leeway which caused water to go spill onto deck. The actual tests that were undertaken are shown in Table 4. Note in Table 4 that V1 corresponds to the rounded hull, V2 to the wide Vee hull, and V3 to the narrow Vee hull.

Table 1 Tests done from 2 July – 5 July in the Newcastle Towing tank on slender hulls

Yaw/Speed	0.4 m/s			0.8 m/s			1.0 m/s	1.2 m/s			1.6 m/s	
0 degrees	V1	V2	V3	V1	V2	V3		V1	V2	V3	V1	V2
4 degrees	V1		V3	V1		V3		V1		V3	V1	
8 degrees	V1	V2	V3	V1	V2	V3		V1	V2	V3		V2
12 degrees			V3			V3				V3		
16 degrees	V1	V2	V3	V1	V2	V3		V1	V2	V3		V2
24 degrees	V1	V2		V1	V2		V2	V1	V2			

Analysis of fixed sink and trim results

Description of testing procedures

Normal tank testing procedures were used to carried out the tests, such as waiting for sufficient time for the water to settle between runs, checking the waterline height each day after skimming, zeroing the load cells, repeating the same test from the last run of the previous day to the first run of the following day, and repeating runs were the results looked questionable.

Drag, lift, resistance and side force as a function of speed

It is common to plot tank test results as a function of model speed, or Froude number. Here the force results are plotted against model speed. The test speeds were nominally 0.4, 0.8, 1.2 and 1.6 m/s. These correspond to Froude numbers of

0.12, 0.23, 0.35 and 0.47. Drag force is plotted against speed in Figure 8 for all three models. Several features are apparent in the figure. The narrowest model, V3 has the lowest drag for a given speed, followed by the wider Vee model (V2) and the rounded model (V1). The drag increases as speed increases, as expected, and the drag increases as the leeway angle is increased, although the V2 and V3 models have very similar drag when yawed at 16°. Drag coefficient is plotted against speed in Figure 9. Here it is evident that the coefficients are essentially constant over the speed range of the tests. It is more evident that yawing the model to produce leeway gives a significant increase in the drag coefficient as expected. The V3 model was not tested at a leeway angle of 24°. Note that the reference area here is the projected immersed side area, which is the same for the three models, and is 0.0488 m^2.

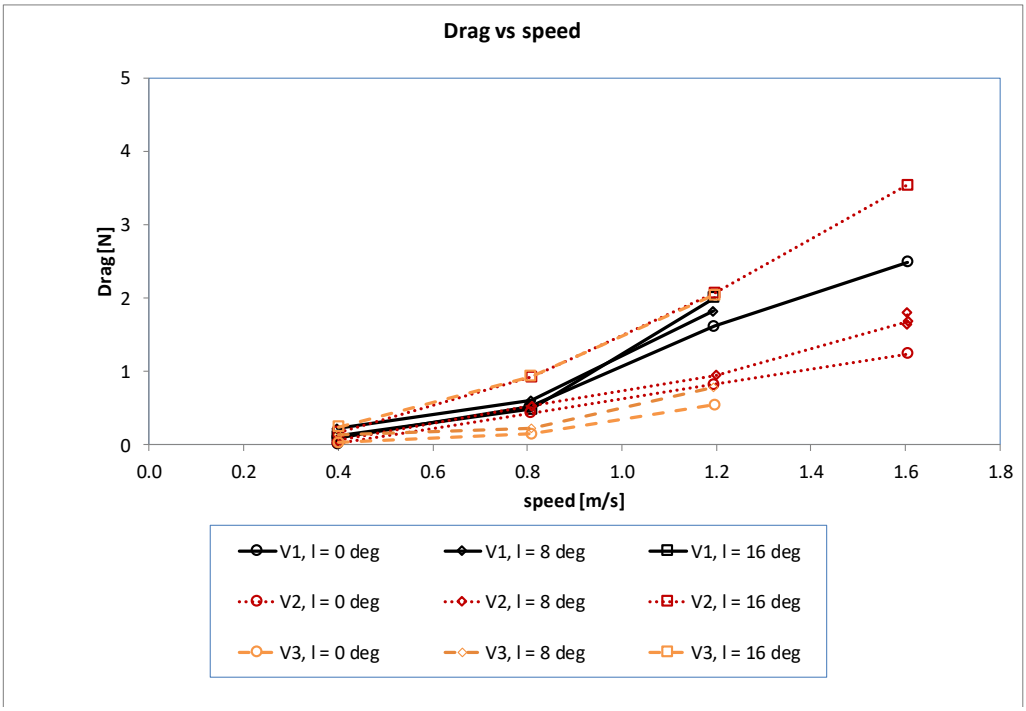

Figure 8 Fixed sink & trim, drag versus speed for all three models

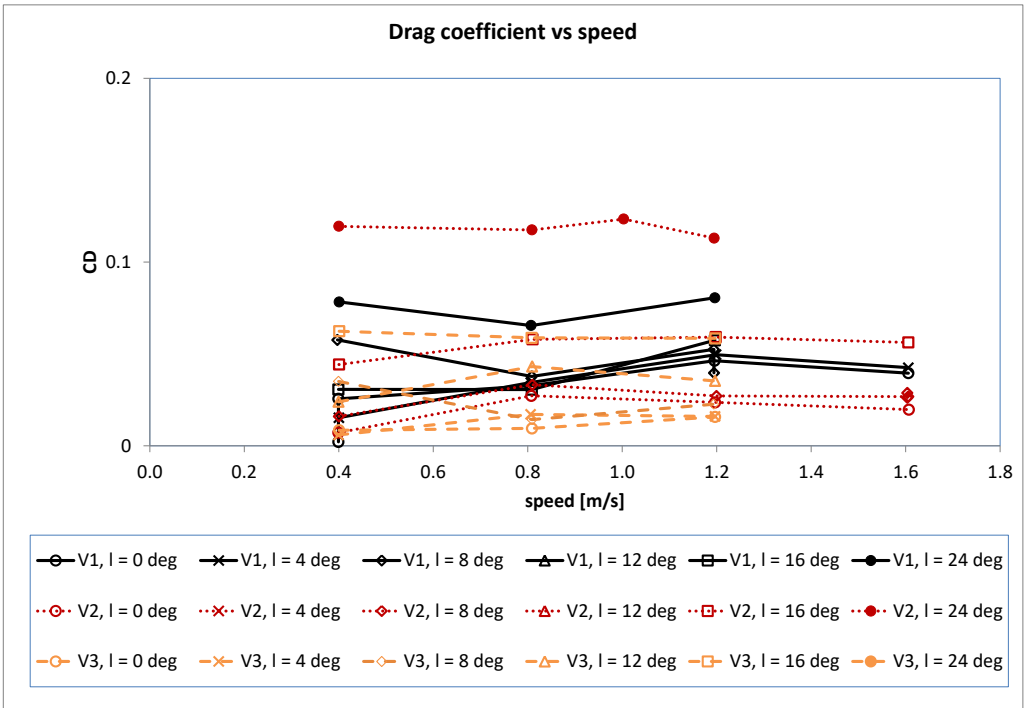

Figure 9 Fixed sink & trim, drag coefficient versus speed for all three models

Resistance coefficient is plotted against speed in Figure 10. One might expect the resistance and drag coefficient plots to look similar, and indeed this is the case for the low leeway angles, but for larger angles the significant amount of lift that is generated (of order twice the drag force) has a component that subtracts from the resistance, which lowers it significantly. This also has the effect of reordering the results. The rounded V1 model (black solid lines), which is not so good at generating lift, has the highest resistance, and conversely the narrow V3 model (yellow dashed lines) has the lowest resistance coefficient.

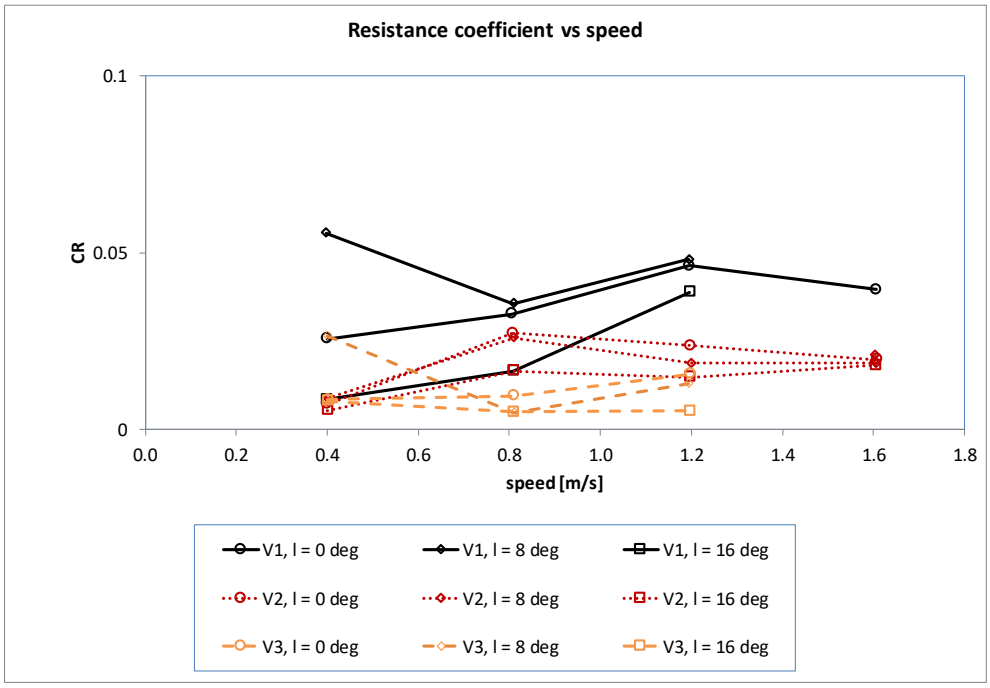

Figure 10 Fixed sink & trim, resistance coefficient versus speed for all three models

The lift and side-force coefficients are the primary foci of this work, and lift force is plotted against speed in Figure 11. It can be seen that the lift force is approximately twice the drag force, and that as the models become narrower, they become more efficient at generating lift. The V1 model at 0° shows a small negative lift force at a speed of 1.6 m/s. This is due to experimental error, possibly a very small angle misalignment of the model.

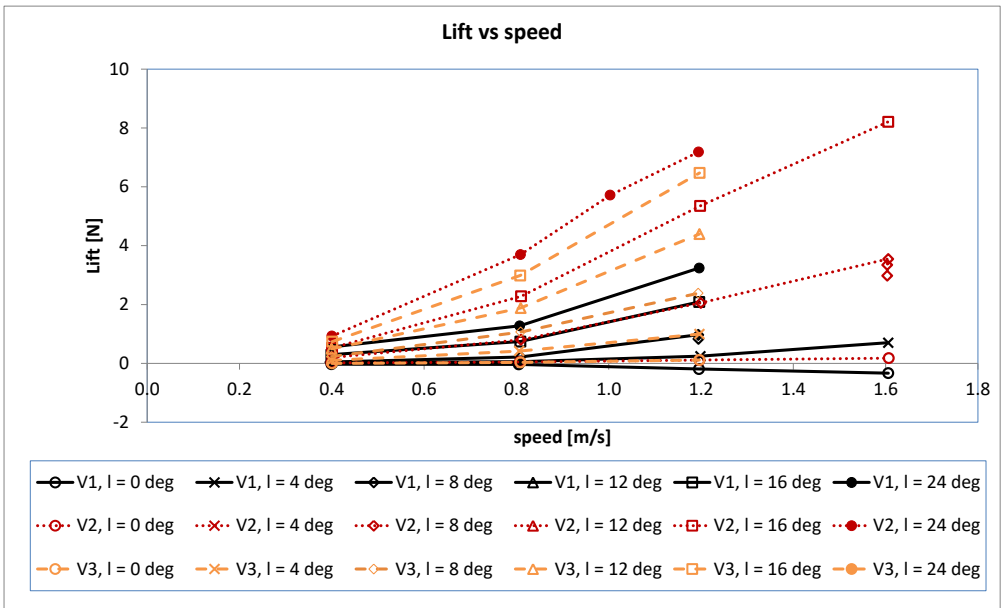

Figure 11 Fixed sink & trim, lift versus speed for all three models

The lift coefficients are shown in Figure 12, and as observed for the drag coefficients, the lift coefficients are also relatively unaffected by the speed over the range tested, although there is perhaps a slight trend to smaller coefficients as speed is increased. It is also evident that there is a much larger increase in lift coefficient between the rounded model V1 and the wide Vee model V2, with a smaller difference to the V3 model.

The side force coefficient is plotted against speed in Figure 13, where the reference area is *A*, the immersed projected side area which is the same for all models. It can be seen that this figure is similar to Figure 12. The results are ordered the same, and the main difference is that the side force coefficient is a little larger than the lift coefficient for the larger leeway angles, as the drag has a component which adds to the side force. The side force coefficients are also relatively unaffected by test speed. In both Figures 12 and 13, the ranking of lift and side-force from the three lines can been seen by studying the lines with the open square symbols (16° leeway). Similar to the CFD results, these experimental results show that having a narrower hull enables more lift of side-force to be generated for a given leeway angle.

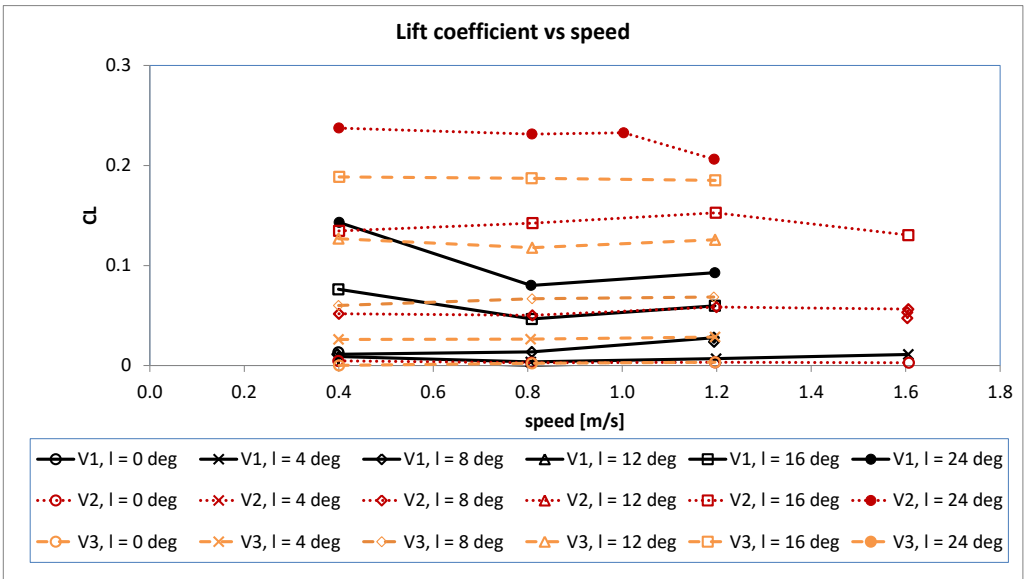

Figure 12 Fixed sink & trim, lift coefficient versus speed for all three models

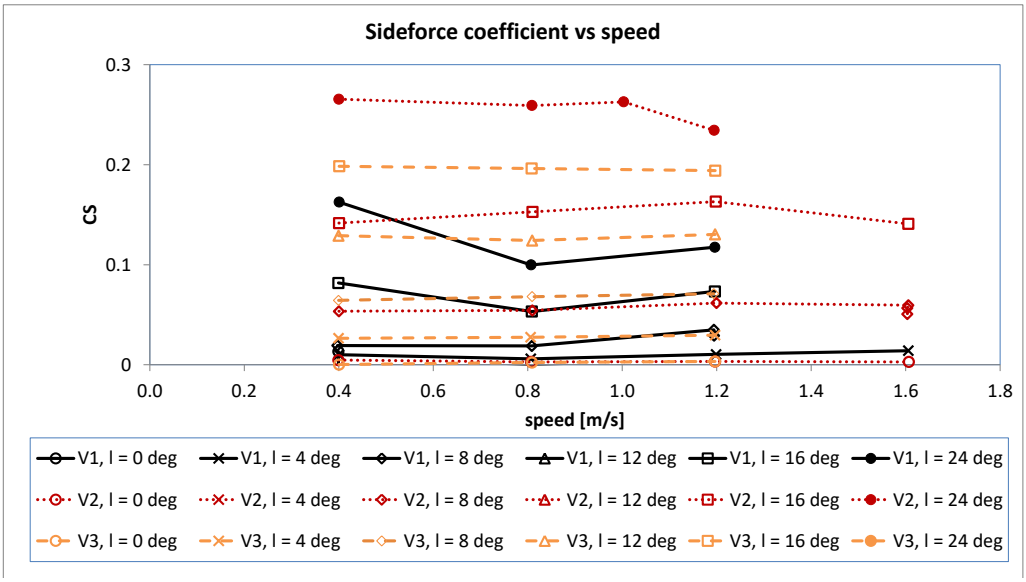

Figure 13 Fixed sink & trim, side force coefficient versus speed for all three models

Drag, lift, resistance and side force as a function of leeway angle

Since one of the objectives of carrying out this work was to obtain better estimates of side force for Polynesian sailing vessels as a function of leeway angle, the results are also shown in that manner. This presentation also enables them to be compared with the CFD predictions available in Boeck 2010, which were carried out at a speed of 3 knots (1.5433 m/s) for several leeway angles.

Drag force is plotted against yaw in Figure 14 for all three models. Here it can be seen that drag increases with increasing yaw angle for all three models, and that the rounded V1 model has the highest drag for a given yaw, followed by the moderate V2 model and by the narrowest V3 model. The drag coefficient is plotted against leeway angle in Figure 15. Although the variation in the results indicates some effect of experimental error, it is clearly evident that the three models show different trends. The drag coefficient for the rounded V1 model does not increase as quickly with yaw angle as does the drag coefficient for the V2 model, and the narrowest V3 model shows the most rapid increase in drag coefficient with yaw angle. Hence at a yaw angle of 0°, the drag coefficient is highest for the V1 model and lowest for the V3 model, but at a yaw angle of 16° the order is reversed. The V3 model was not tested at a yaw angle of 24°, which perhaps is unfortunate, as it might have shown up this effect even more clearly. All models had the same drag coefficient at an angle of about 7°.

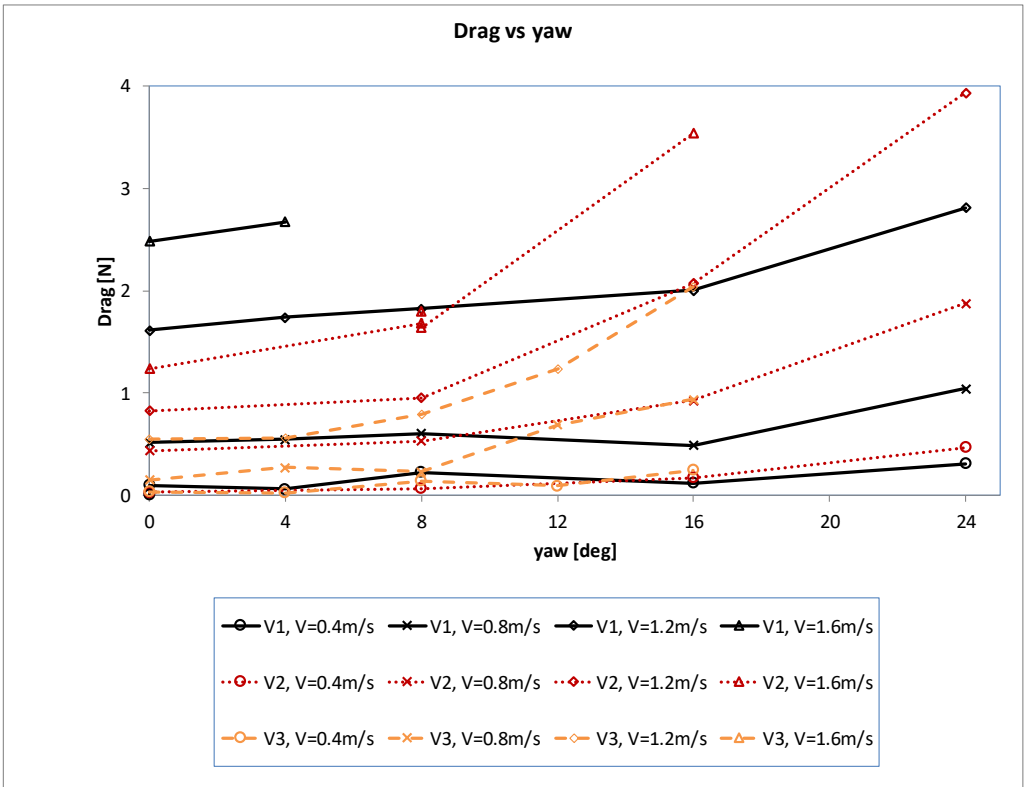

Figure 14 Fixed sink & trim, drag versus leeway angle for all three models

Figure 15 also shows the CFD predictions for drag coefficient as lines without symbols. Boeck 2010 and 2012 used CFD to predict the drag of a full-scale vessel at a speed of 1.543 m/s, and for coarse increments of leeway angles of 0, 5, 10 and 15°, for all the three hull shapes. Boeck's data were fitted by second order polynomial functions and used to plot the lines shown. Note that there is a disparity in the CFD and tank Reynolds numbers, and this point is returned to later when the tank coefficients are scaled to full-scale Re using the Prohaska-Hughes method. It can be seen that the CFD predictions are low for the rounded V1 model, but the trend of increase with yaw angle is represented in a similar fashion both in the CFD and model tests. There is reasonable agreement between the CFD predictions and the model drag coefficient values for the tests at a speed of 0.4 m/s for the V2 model. Interestingly, the Froude number corresponding to a model test speed of 0.4 m/s is 0.12, which converts to a speed of 1.26 m/s at full-scale. This model result is at the closest Froude number to the CFD predictions done at a speed of 1.543 m/s. There is fairly good agreement between the model and CFD results for the narrow V3 model over the range of leeway angles that were tested up to 16°.

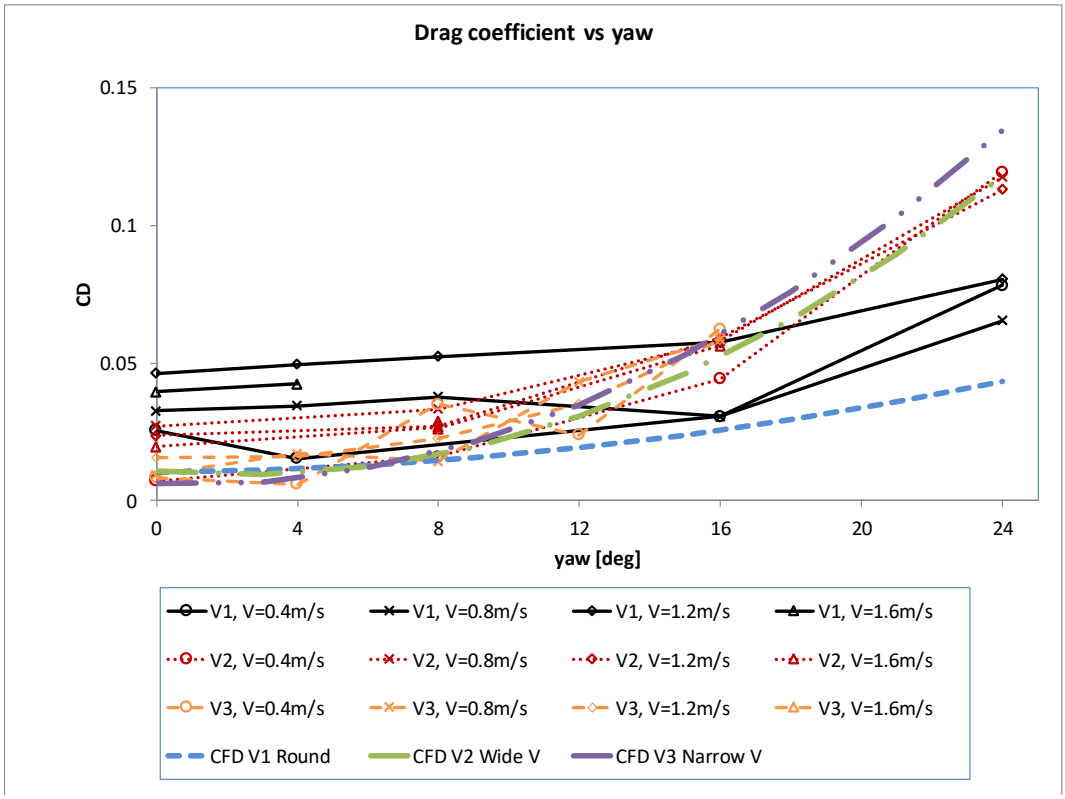

Figure 15 Fixed sink & trim, drag coefficient versus leeway angle for all three models, and comparison with CFD predictions.

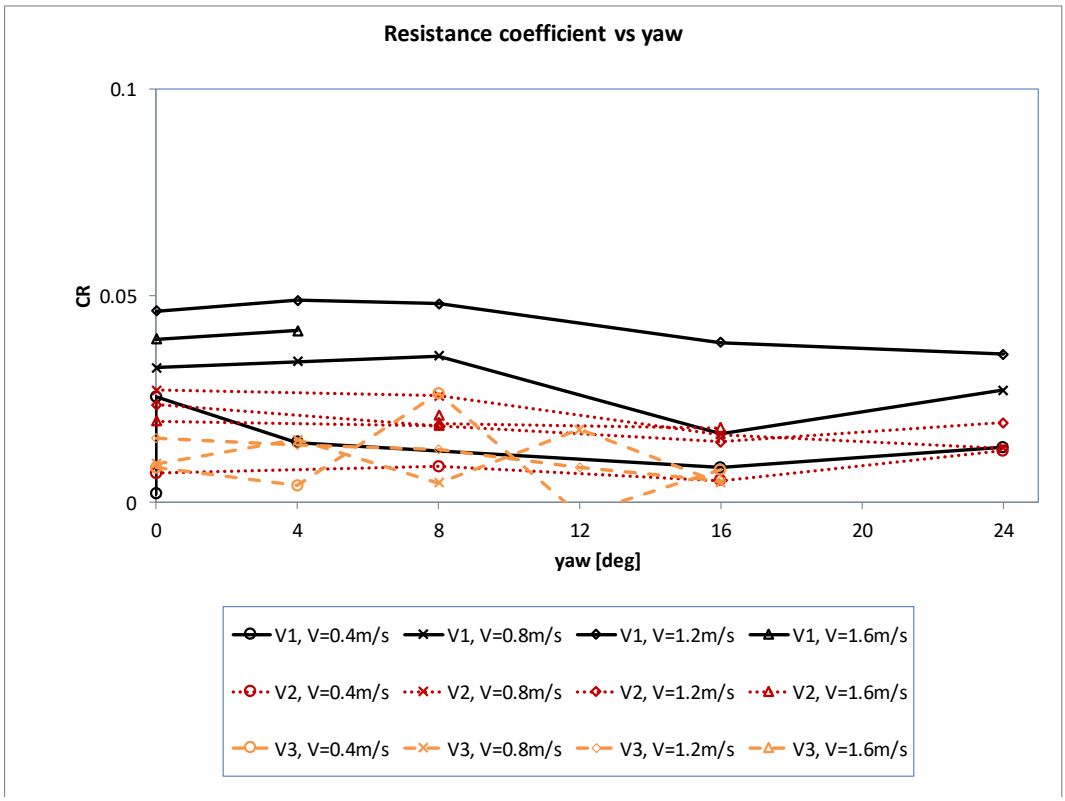

Figure 16 Fixed sink & trim, resistance coefficient versus leeway angle for all three models

The resistance coefficient is plotted against leeway angle in Figure 16. There is a rather striking difference between the drag and resistance coefficient plots, which may seem rather surprising. The resistance coefficients are generally lower than the drag coefficients, for the same reason as discussed in the previous section, that the lift force subtracts from the resistance, particularly at the higher leeway angles, where it can be seen in Figure 16 that the coefficients actually decrease with increasing yaw angle. The second major difference with the drag coefficient plots is that the resistance coefficient is always highest for the rounded V1 hull, and lowest for the narrow V3 hull, across the entire yaw angle range.

The lift force is plotted against leeway angle in Figure 17 for all three models. It is evident that lift force increases with increasing yaw angle, and that the narrowest V3 model is the best at producing lift, and the rounded V1 model is the worst at producing lift. Turning these lift forces into coefficients, as shown in Figure 18, puts the lines into clear groups, with it even more evident how a rounded hull is much worse at producing lift compared to having a narrow Vee. The effect of model speed can be seen to have a relatively minor effect on the coefficients for the V2 and narrow V3 model, but a slightly larger effect on the rounded V1 model.

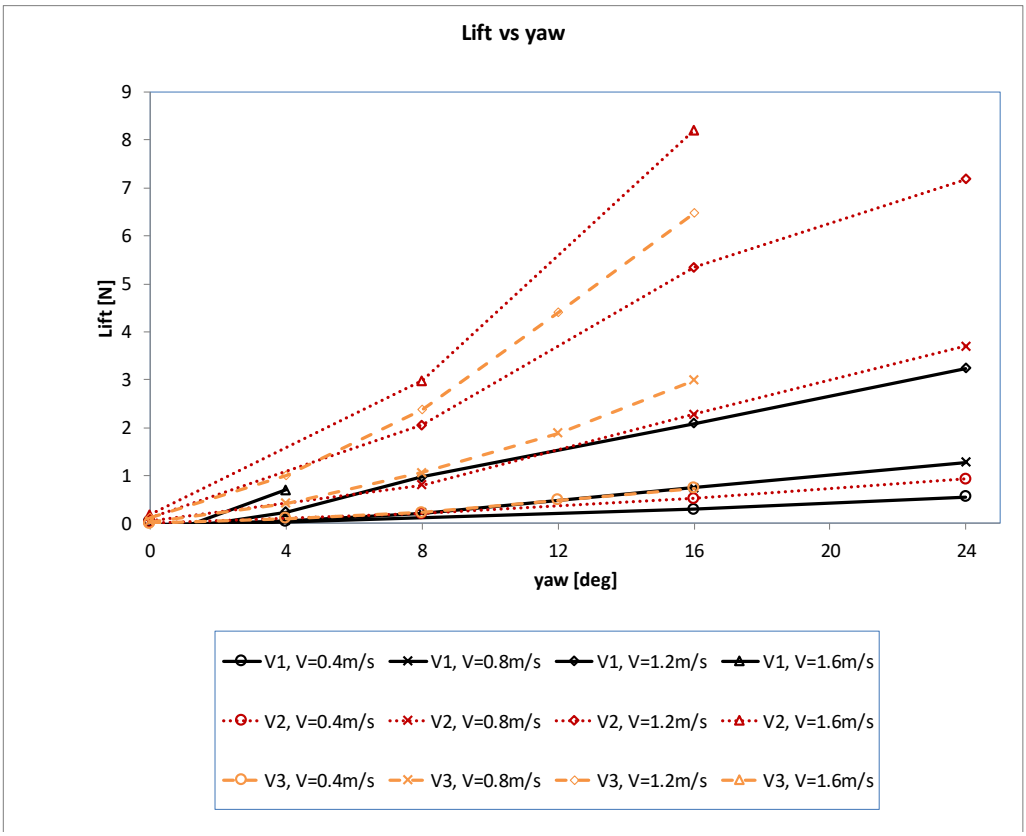

Figure 17 Fixed sink & trim, lift versus leeway angle for all three models

The CFD predictions of the lift coefficient from the work of Boeck 2010, 2012 are also plotted in Figure 18. Boeck carried out simulations on full-scale vessels of identical shape to the present tank test models, at a speed of 3 knots (1.5433 m/s), for a range of yaw angles. His data have been fitted to second order polynomials, and plotted as shown. It is clearly evident that the agreement is extremely good, and that the CFD predictions lie within the band of experimental results for each of the three models, up to a leeway angle of 16°, and beyond that angle, the predictions are still rather good.

The side force coefficients are plotted in Figure 19. These can be seen to look almost identical to the lift coefficients in Figure 18. There are groups of lines bunched together for each of the test models showing that the coefficients are only weakly dependent on speed.

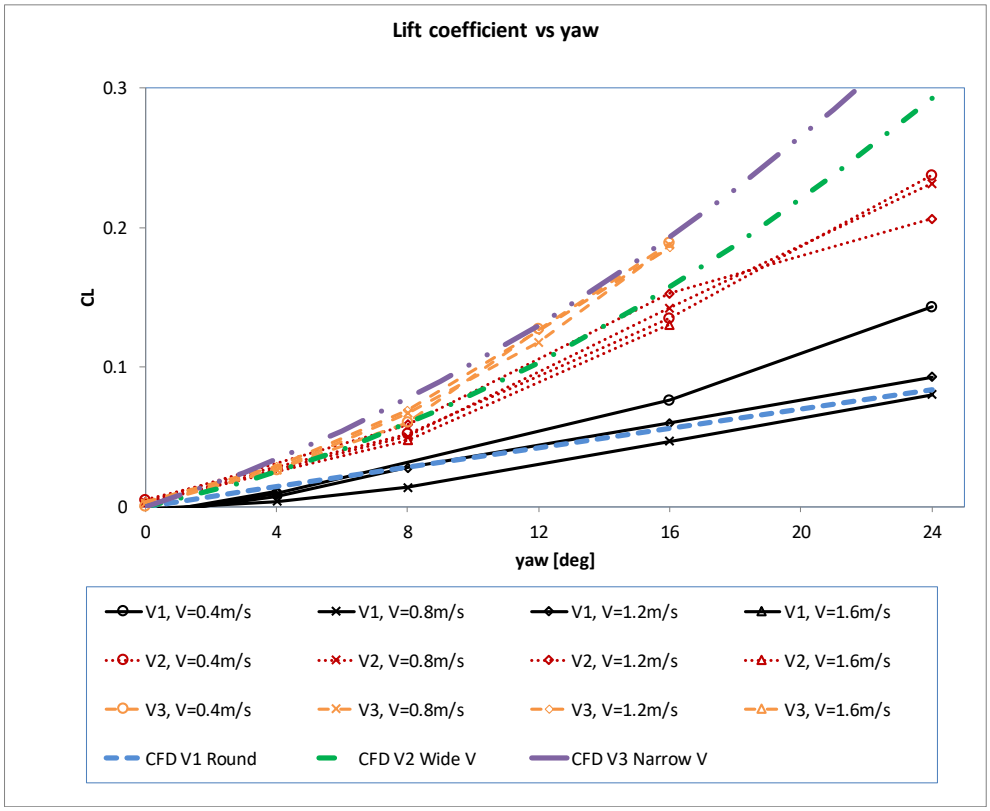

Figure 18 Fixed sink & trim, lift coefficient versus leeway angle for all three models, and comparison with CFD predictions Boeck 2010, 2012

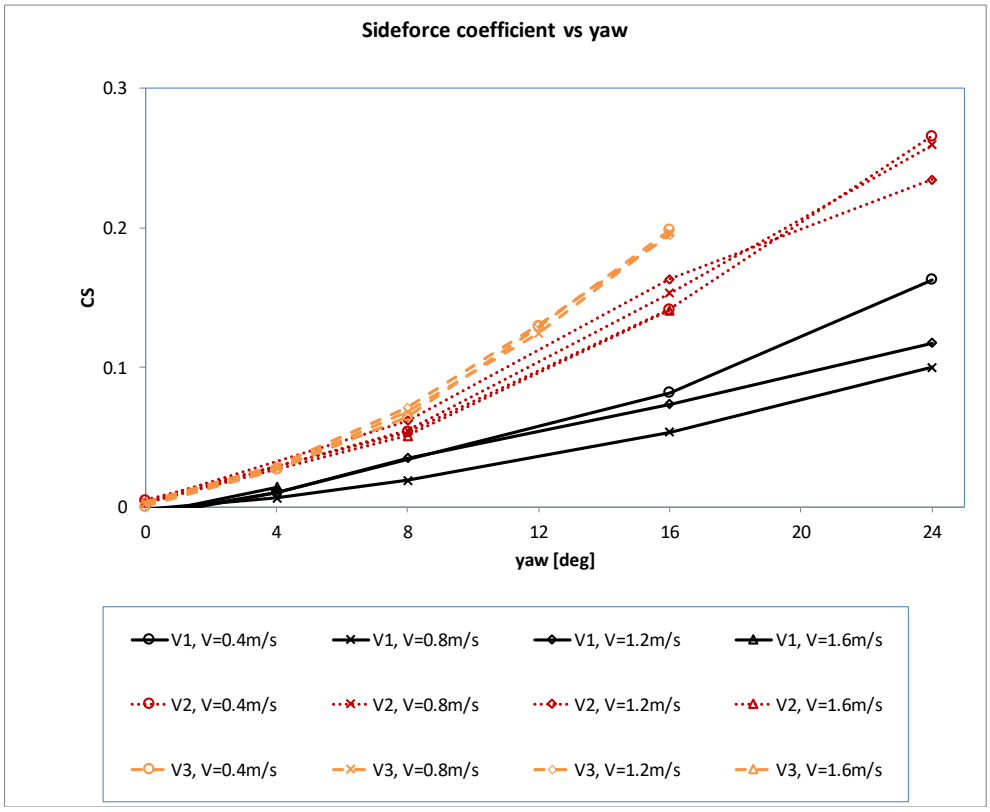

Figure 19 Fixed sink & trim, side force coefficient versus leeway angle for all three models, and comparison with CFD predictions Boeck 2010, 2012

It should be noted at this point that the CFD simulations were carried out at full-scale, i.e. at a Reynolds number of about 20 million, whereas the present tank results were carried out at a Reynolds numbers in the range 0.5 to 2 million, or more than 1 order of magnitude less. Whereas there are well developed procedures for scaling tank resistance results to full-scale Reynolds numbers, it is not clear that there are similar procedures for scaling the lift or side force results. Hence the comparisons shown in Figures 18 and 19 are for different CFD and tank model Reynolds numbers. No Reynolds number scaling corrections have been applied to the lift and side force results presented in the paper. The effect of Reynolds number on the drag is discussed in the next section.

Scaling of drag coefficients from model to full-scale

When predicting full-scale drag using model tests, the test results have to be scaled, or extrapolated, from model to full-scale. The method used in the present tests is due to Hughes, and was introduced in the 1950s, and later adopted by the International Towing Tank Conference (ITTC). Details on the method can be found in ITTC 7.5-02-01-03, 2002 and ITTC 7.5-02-02-01, 2002, Rev. 01. A summary description is provided herewith.

The basis of the approach is that the resistance is the sum of frictional resistance which scales with Re, and residuary resistance which scales with Fr, since it mainly consists of wave-making resistance, as proposed by Froude, and given in Eq. (6).

$$C_T = C_F(Re) + C_R(Fr). \tag{6}$$

Hughes proposed the form factor approach given by Eqs. (7) and (8),

$$C_T = C_V + C_W, \text{ and} \tag{7}$$
$$C_V = (1+k)C_{F0}\ , \tag{8}$$

where $(1+k)$ is the form factor, which depends on hull form (i.e. shape), C_{F0} is the skin friction coefficient based on flat plate results, C_V is a viscous coefficient taking account of both skin friction and viscous pressure resistance, and C_W is the wave resistance coefficient.

k is generally small, say 0 to 0.2. The trend of C_{F0} with Re is the "correlation line" adopted by the ITTC in 1957. It incorporates some three-dimensional effects and is given by Eq. (9).

$$C_{F0} = \frac{0.075}{(\log_{10} Re - 2)^2}. \tag{9}$$

The full-scale drag coefficient is found by assuming that the wave drag coefficients are the same at model and full-scale at the same Reynold number, and that the form factor is the same in both model and full-scale. The skin friction coefficient terms is evaluated using the ITTC correlation line formula using an appropriate Reynolds number. In equation form, this can be written as in Eqs. (10) and (11).

$$C_{Tms} = C_{Vms} + C_{Wms} = (1+k)C_{F0ms} + C_{Wms} \tag{10}$$
$$C_{Tfs} = C_{Vfs} + C_{Wfs} = (1+k)C_{F0fs} + C_{Wfs} \tag{11}$$

where the model and full-scale form factors are the same.

The full-scale wave drag can be found from the model results using Eq. (12).

$$C_{Wms} = C_{Wfs} = C_{Tms} - (1+k)C_{F0ms} \tag{12}$$

Therefore the total full-scale drag can be written as in Eq. (13).

$$C_{Tfs} = (1+k)C_{F0fs} + C_{Tms} - (1+k)C_{F0ms} \tag{13}$$
$$C_{Tfs} = C_{Tms} - (1+k)\left(C_{F0ms} - C_{F0fs}\right), \tag{14}$$

finally giving Eq. (15).

$$C_{Tfs} = C_{Tms} - (1+k)\left(\frac{0.075}{(\log_{10} Re_{ms} - 2)^2} - \frac{0.075}{\left(\log_{10} Re_{fs} - 2\right)^2}\right) \tag{15}$$

The form factor is determined from the model results by postulating that the wave drag coefficient is proportional to Froude

number to the power 4, and for conducting tests at low Fr say 0.1 to 0.2, then the straight line plot of C_{Tms}/C_{F0ms} versus Fr^4/C_{F0ms}s will intersect the ordinate ($Fr = 0$) at $(1+k)$, and the slope, say A, can also be determined. This is called a Prohaska plot.

It is described in Eq. (16).

$$C_{Tms} = (1+k)C_{F0ms} + C_{Wms} = (1+k)C_{F0ms} + A \times Fr^4, \tag{16}$$

finally resulting in Eq. (17).

$$\frac{C_{Tms}}{C_{F0ms}} = (1+k) + A \times \frac{Fr^4}{C_{F0ms}} \tag{17}$$

The measured tank drag data for all three models and for all leeway angles have been analysed using the method explained above. The Prohaska plots are shown in Figures 20, 21 and 22. It is evident that there is quite a lot of noise in the data. As mentioned previously, the drag values for these small models were quite low (for example at a towing speed of 0.4 m/s the drag was of order 0.1 N) so the accuracy was not as good as it would have been with larger models. It is also evident that the form factor appears to increase as the leeway angle increases. This is probably an artefact of the method, which assumes that there is no flow separation. Indeed, there is likely to be flow separation when the model is yawed, particularly for the V2 and V3 models.

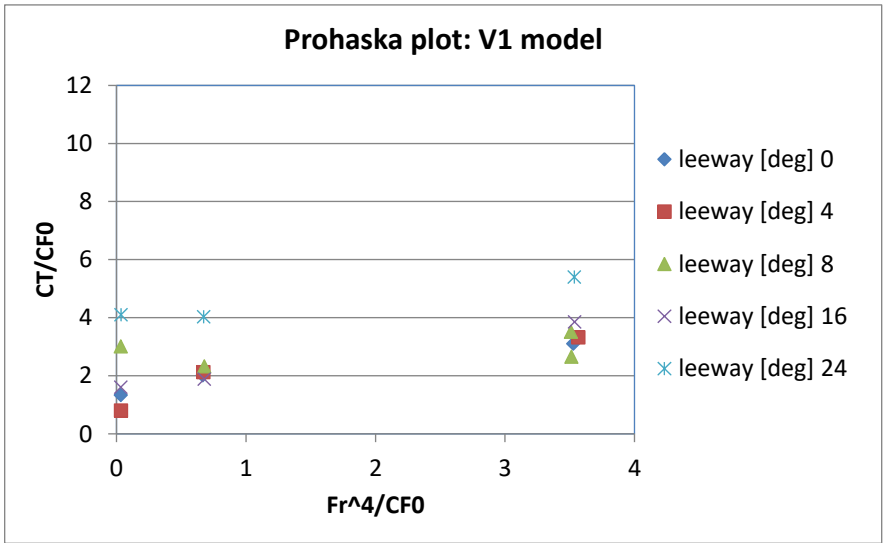

Figure 20 Prohaska plot to determine the form factor for the V1 model

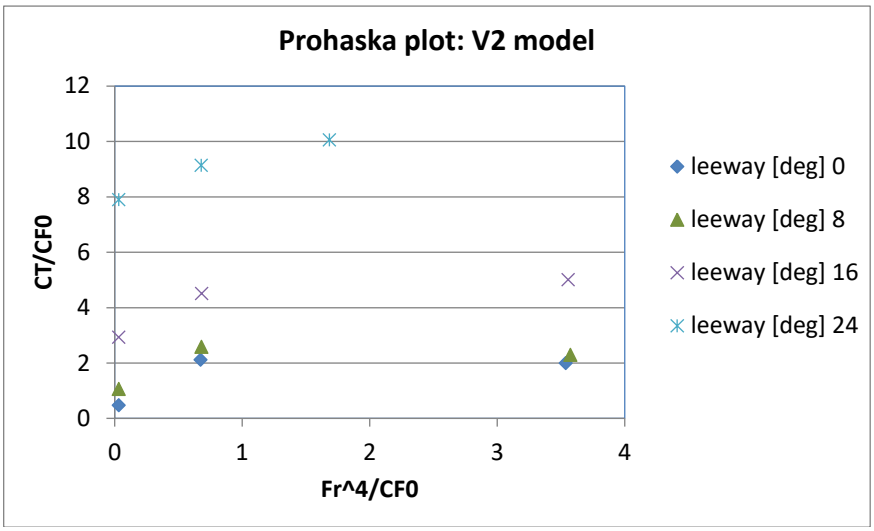

Figure 21 Prohaska plot to determine the form factor for the V2 model

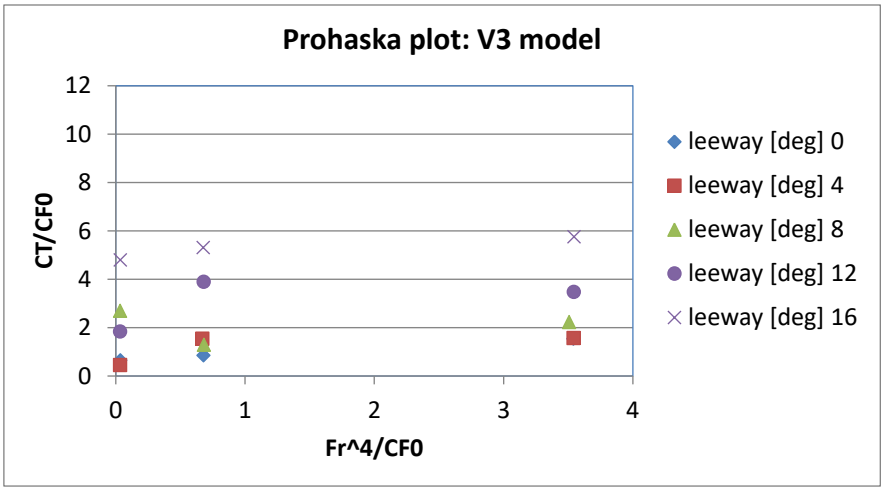

Figure 22 Prohaska plot to determine the form factor for the V3 model

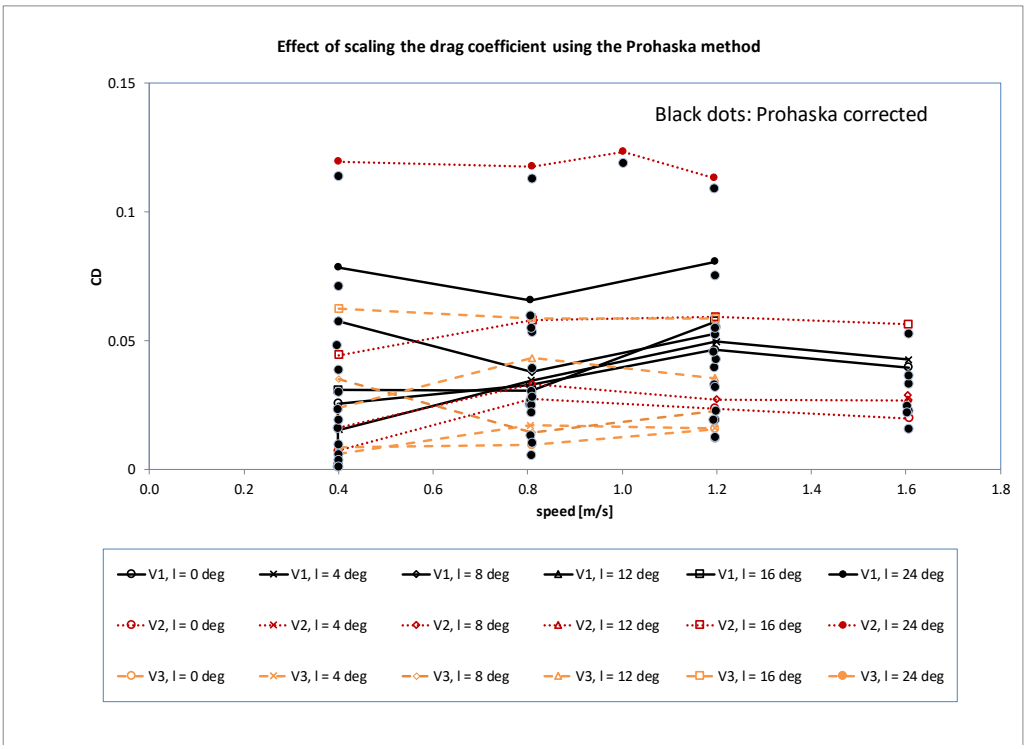

Figure 23 Plot of drag coefficients for all models showing the slight reduction in values (shown by the black dots) when the data are corrected using the Prohaska-Hughes method.

The form factor appears to decrease as the models become narrower. Estimates of the form factor for the V1, V2 and V3 models are 1.3, 1.1 and 1.0 respectively based on fitting straight lines to the data, although they cannot be determined with much accuracy. Nonetheless, these values have been used to recalculate the drag coefficients for full scale. These full-scale coefficients have been plotted on Figure 23 as black dots. They all lie slightly below the model scale values. Although the value of the correction varied somewhat, it was found to result in a reduction of 0.005 on average, which although not large, is significant.

CONCLUSIONS

A CFD study with ANSYS-CFX using three different hulls was carried out as suggested by the first author and it showed that sharper Vee sections were better at generating lift and side-force than a rounded hull. The purpose of the present tests was to investigate whether such behaviour could also be observed in physical testing.

Three models were manufactured and were tested in the Towing Tank at Newcastle University in July 2013 with fixed sink and trim.

The drag coefficients were corrected from the tank Reynolds number of about 1 million to full-scale which is about 20 million using the Prohaska method. It was found that the correction resulted in a reduction of drag coefficient of the order of 0.005. this value is relatively small, and is probably of the same order, or in fact smaller, than the experimental error.

It was found that there was good agreement between the side-force predicted by CFD and experimentally determined values from tank test results on three different models. The predictions from the CFD that narrower Vee shaped hulls would generate more side-force when at leeway than a rounded hull was confirmed by the present tank test results.

ACKNOWLEDGEMENTS

This research was carried out as part of the Sailing Fluids project funded jointly by the EU and by NZ. The grant details are as follows. EU - Call: FP7-PEOPLE-2012-IRSES, Funding scheme: MC-IRSES (International Research Staff Exchange Scheme (IRSES)), Proposal number : 318924, Proposal acronym : SailingFluids. NZ - IRSES Application 2012-318920-SAILING FLUIDS funded by the Royal Society of New Zealand. The first author was assisted in carrying out the towing tank tests by Alexander Blakeley, Joshua Taylor, and Nick Velychko whose contributions are gratefully acknowledged. The technical support provided by the Newcastle University technical staff in the laboratory is also gratefully acknowledged.

REFERENCES

Newcastle towing tank,
https://www.ncl.ac.uk/engineering/about/facilities/marineoffshoresubseatechnology/hydrodynamics/#towingtank
accessed 20/12/2018.

Boeck, F., "Side force generation of slender hulls", *Study Thesis*, TU Berlin, Germany, 2010.

Boeck, F., Hochkirch, K., Hansen, H., Norris, S., Flay, R.G.J., "Side force generation of slender hulls – influencing Polynesian canoe performance", Proc. 4th High Performance Yacht Design Conference, Auckland, New Zealand 12-13 March 2012.

ITTC – Recommended Procedures and Guidelines 7.5-01 -01-01 Page 5 of 6 Model Manufacture Ship Models Effective Date 2002 Revision 01

ITTC Recommended Procedures 7.5-02-01-03, 2002. '*Testing and Extrapolation Methods, General Density and Viscosity of Water' ITTC Recommended Procedures 7.5-02-01-03.* s.l., ITTC.

ITTC – Recommended Procedures and Guidelines 7.5-02 -02-01 Testing and extrapolation methods resistance. Resistance Test. Effective Date 2002, Revision 01.

Wong, H.L., "Slender ship procedures that include the effects of yaw, vortex shedding and density stratification", *Thesis*, University of British Columbia, Vancouver, Canada, 1994.